

Fluorescence spectroscopy enhancement on photonic nanoantennas

Jérôme Wenger^{1*}

¹Aix Marseille Univ, CNRS, Centrale Marseille, Institut Fresnel, UMR 7249, Marseille, France

* Corresponding author: jerome.wenger@fresnel.fr

1 Introduction and motivation

Despite the significant progress in single molecule fluorescence microscopy made over the last two decades, the efficient detection of a single molecule remains a major goal with applications in chemical, biochemical and biophysical analysis [1, 2]. The phenomenon of light diffraction appears as a main physical limiting factor. Indeed, there is a huge size mismatch between a single molecule (below 5 nm) and the wavelength of light (around 500 nm). This size mismatch prevents the efficient interaction between an incoming light beam from a conventional optical microscope and a single fluorescent molecule, so the net detected fluorescence signal from a single molecule (ultimately defining the sensitivity and dynamic temporal resolution achievable) remain limited [3].

Additionally, conventional optical microscopes are restricted to conditions of low density (or concentration) of fluorescent molecules [1, 4]. In order to isolate a single molecule in the diffraction-limited volume of a confocal microscope, the concentration range must be typically in the pico to nanomolar range. However, a large majority of enzymes and proteins requires concentrations in the micro to millimolar range to reach relevant reaction kinetics and biochemical stability. Monitoring single molecules at high physiological concentrations thus requires overcoming the diffraction limit to confine light in a nanometer spot of volume in the zepto- (10^{-21}) or atto- (10^{-18}) liter range, more than three orders of magnitude below the femtoliter volumes achieved with confocal microscopes [5, 6].

Confining light to the nanoscale can be achieved thanks to optical antennas [7]. Optical antennas are generally metallic nanostructures with dimensions much below the wavelength of light [8, 9]. Like their radiofrequency counterparts, optical antennas convert propagating radiation into localized energy and vice-versa [7]. This opens new routes to enhance and control the emission from a single fluorescent emitter by improving the light-matter interaction between a single fluorescent molecule and the incoming beam, leading to the phenomenon of antenna-enhanced fluorescence emission [10, 11, 12]. Over thousand-fold enhancement of the single molecule fluorescence signal was reported

with lithographically fabricated gold nanogap antennas [13, 14, 15], with dimers of gold nanoparticles assembled with DNA origami [16, 17] and with a single gold nanorod [18, 19].

In this Chapter, we will briefly introduce the key concepts to understand the phenomenon of fluorescence enhancement with optical nanostructures. The equations will remain simple, with the major goal to illustrate the different effects at play. Next we will provide an overview of different recent approaches to enhance single molecule fluorescence with plasmonic and non-plasmonic nanoantennas. Lastly, we will describe three main biochemical applications that this technique opens.

2 Brief theoretical background: the physics of fluorescence enhancement

In order to understand the phenomenon of enhanced fluorescence in the vicinity of a nanostructure, one has to go back to the representation of the quantum emitter as a two energy levels system. Γ_{rad} and Γ_{nr} are the rate constants for radiative and non-radiative transitions from the excited singlet state to the ground state. The total de-excitation rate from the excited singlet state is then $\Gamma_{tot} = \Gamma_{rad} + \Gamma_{nr}$, and corresponds to the inverse of the excited state fluorescence lifetime $\tau = 1/\Gamma_{tot}$. With these notations, the ratio of the radiative rate to the total decay rate (probability of de-excitation transition accompanied with the emission of a photon) is defined as the fluorescence quantum yield $\phi = \Gamma_{rad}/\Gamma_{tot} = \Gamma_{rad}/(\Gamma_{rad} + \Gamma_{nr})$. Lastly, the excitation rate constant is noted σI_e , with σ being the excitation cross-section and I_e the local excitation intensity.

Under steady-state conditions, the fluorescence brightness (or count rate) per molecule Q can be written as [20]

$$Q = \kappa \phi \frac{\sigma I_e}{1 + I_e/I_s}. \quad (1)$$

Here κ denotes the light collection efficiency of the optical microscope apparatus, and $I_s = \Gamma_{tot}/\sigma$ is the so-called saturation intensity. Generally the experiments are performed in the weak excitation regime well below fluorescence saturation (corresponding to $I_e \ll I_s$), so as to avoid photobleaching the emitters and introducing other photodamages to the photonic nanostructure. In this regime, the brightness Q reduces to a simpler form:[21]

$$Q = \kappa \phi \sigma I_e. \quad (2)$$

We retrieve here that the fluorescence rate per molecule is proportional to the collection efficiency, the quantum yield, and the excitation intensity.

In the presence of the optical nanoantenna, all the transition rates are potentially modified (here, we note with a * the quantities modified by the nanoantenna). The local excitation intensity becomes

I_{exc}^* and can be significantly greater than the incoming intensity by taking advantage of the sub-wavelength confinement of light at the nanoantenna (similar to the lightning rod effect) which can be further additionally enhanced by the plasmonic resonances of the nanoantenna. Locally, the excitation intensity I_{exc}^* can thus overcome I_{exc} by more than a hundred fold. The radiative decay rate is also enhanced (as a consequence of the reciprocity theorem) and becomes Γ_{rad}^* .

A major challenge in enhancing fluorescence with metal nanostructures comes from the presence of additional losses (with rate constant noted Γ_{loss}^*) which are introduced by the presence of the metal nearby. These losses account for non-radiative energy transfer to the free electron gas in the metal, whose energies are further dissipated by Joule (ohmic) losses. Consequently, the total decay rate with the nanostructure becomes $\Gamma_{tot}^* = \Gamma_{rad}^* + \Gamma_{nr} + \Gamma_{loss}^*$. It is greater than the initial decay rate Γ_{tot} so the net photodynamics decay is accelerated by the presence of the nanoantenna. However, this increase in the total decay rate $\Gamma_{tot}^*/\Gamma_{tot}$ must *not* be confused with the fluorescence enhancement (which is the ratio of the brightnesses per emitter Q^*/Q). Indeed, a significant fraction of the total decay rate Γ_{tot}^* can be due to non-radiative losses Γ_{loss}^* which lead to a decrease of the apparent fluorescence brightness also known as quenching. Said differently, a fluorescent emitter can experience an ultrashort lifetime near a nanoantenna, corresponding to an increased total decay rate Γ_{tot}^* but this can be essentially a consequence of strong non-radiative losses damping all the energy away from the radiative transitions. This situation is typically found for a fluorescent molecule in very close (below 5 nm) proximity to a small gold nanoparticle of diameter below 15 nm: the gold nanoparticle acts here as a fluorescence quencher. Therefore, in any fluorescence enhancement experiment with a nanoantenna, a delicate balance must be found between enhancing the radiative decay rate Γ_{rad}^* without introducing too many losses Γ_{loss}^* . As a side note, we point out that the situation is conceptually different in surface enhanced Raman scattering (SERS), where the scattering is a nearly instantaneous process and where there is no finite lifetime of the excited state and no non-radiative decay rates involved. Note also that we assume here that the non-radiative decay rate Γ_{nr} (intrinsic to the fluorescent emitter in use, set by its chemical structure) is not modified by the presence of the metal nanostructure ($\Gamma_{nr}^* = \Gamma_{nr}$). This assumption will simplify the coming equations and is still fully general as the additional losses effects are included in the term Γ_{loss}^* .

With the previous expression of the brightness per emitter Q , the fluorescence enhancement factor η_F is then simply defined as the ratio of brightnesses with and without the photonic nanostructure. So the fluorescence enhancement factor writes

$$\eta_F = \frac{Q^*}{Q} = \frac{\kappa^*}{\kappa} \frac{\phi^*}{\phi} \frac{I_{exc}^*}{I_{exc}}. \quad (3)$$

This equation indicates the different relevant quantities to enhance the net fluorescence signal per emitter. The collection efficiency κ^* can be improved by the nanoantenna, directing more optical energy into the collection aperture of the microscope setup. The excitation intensity I_{exc}^* can be

locally enhanced and lastly the quantum yield ϕ^* can be modified.

Improving the apparent quantum yield of the fluorescent emitter deserves more comments to discuss the ratio ϕ^*/ϕ . First, one has to keep in mind that the quantum yield as a probability of radiative transition cannot exceed unity. Therefore, if the emitter has a high initial quantum yield ϕ without the nanostructure (close to 1, like Rhodamine6G molecules for instance), then there is not much that the optical nanoantenna can do to further increase this quantity, and the ratio ϕ^*/ϕ will also be close to one (if it is not reduced to quenching losses). On the contrary, if one starts with a low quantum yield emitter with ϕ on the order of a few percents, then the ratio ϕ^*/ϕ can become apparently very large, thereby improving the net fluorescence enhancement factor η_F . Low quantum yield emitters experience thus the maximum benefit from the presence of the plasmonic nanoantenna. To better represent the influence of the quantum yield and the various transition rates, Eq. (3) can be rewritten

$$\eta_F = \frac{\kappa^*}{\kappa} \frac{I_{exc}^*}{I_{exc}} \frac{\Gamma_{rad}^*}{\Gamma_{rad}} \frac{1}{1 - \phi + \phi(\Gamma_{rad}^* + \Gamma_{loss}^*)/\Gamma_{rad}}. \quad (4)$$

Note that the last ratio in the denominator $(\Gamma_{rad}^* + \Gamma_{loss}^*)/\Gamma_{rad}$ describes the influence of the nanoantenna that is only due to the photonic environment, including ohmic losses and compensating for the intrinsic chemical non-radiative decays Γ_{nr} . This ratio thus corresponds to the net increase in the local density of photonic states (LDOS), sometimes also referred to as the Purcell factor. A high LDOS may thus seem to lower the fluorescence enhancement η_F , but this is counter-balanced by the term $\Gamma_{rad}^*/\Gamma_{rad}$ in the numerator, so a high LDOS generally leads to a higher fluorescence enhancement.

Because of the dependence of the apparent value of the fluorescence enhancement η_F on the initial quantum yield ϕ , comparing between experimental results obtained with different molecular emitters must be made with caution. Extreme fluorescent enhancement factors above a thousand fold have been reported, but all use fluorescent dyes of quantum yield below 10%, and a high fluorescence enhancement factor does not necessarily correlate with a bright photon count rate. To compensate for the dependency on ϕ , the product $\eta_F \times \phi$ has been proposed as a figure of merit for the fluorescence enhancement [22]. This solves one of the problem, but extra care still needs to be taken while comparing results to take into account the influence of other parameters such as the alteration of the collection efficiency and the saturation of the fluorescence process due to large excitation powers [23].

3 Experimental approaches to enhance fluorescence

To overcome the diffraction limit, nanoantenna designs take advantage of sharp curvature radii, nanoscale gaps and plasmonic resonances, using metal nanostructures [7]. A large number of approaches have been investigated over the last decade in order to enhance the fluorescence emission of single molecules and quantum dots [1, 2, 10]. While classical top-down lithography like electron-beam

lithography or focused ion beam milling remains the workhorse for fabricating the nanoantennas, alternative bottom-up strategies using nanoparticle assembly have recently seen much development driven by the seek for a simpler and higher throughput nanofabrication approach.

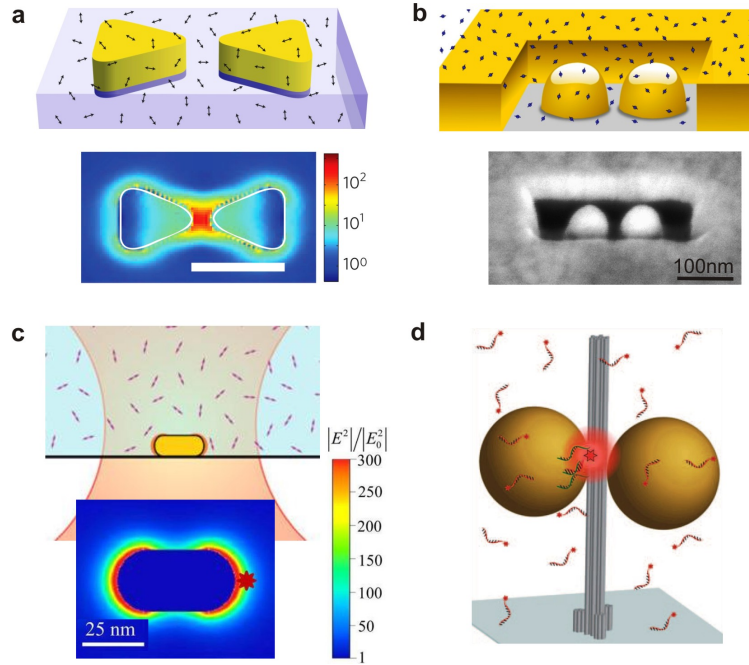


Figure 1: Example of nanoantenna designs for single molecule fluorescence enhancement. (a) Bowtie nanoantenna covered by fluorescent molecules embedded in a PMMA resin [13]. The simulations represent the local excitation intensity enhancement around the nanoantenna (scale bar 100 nm). (b) Antenna-in-box designed for single-molecule analysis at high concentrations [14]. (c) Single gold nanorod for enhanced single molecule detection in solution [19]. The simulations show the near-field intensity map for a 47 x 25 nm gold nanorod. The excitation wavelength is 633 nm, and the excitation is polarized along the long axis of the nanorod. (d) Dimer nanogap antenna assembled by DNA origami [16]. Figures reproduced with permission: copyright (a) Nature Publishing Group 2009, (b) Nature Publishing Group 2013 (c) American Chemical Society 2014 (d) American Association for the Advancement of Science 2012.

3.1 Top-down milling

Electron beam lithography, focused ion beam milling, or deep UV photolithography have a large flexibility in creating a variety of planar antenna designs at specific locations. A nice example is given by the bowtie antenna made of two facing nanotriangles with a 10 nm gap (Fig. 1a) [13, 24]. Plasmonic

coupling between the nanoparticles leads to a local excitation intensity enhancement of 100-fold inside the nanogap region (so-called hot spot) where single fluorescent molecules are randomly deposited. By analyzing all the different single-molecule fluorescence traces on individual nanoantennas, fluorescence enhancement factors up to 1000-fold could be quantified, together with fluorescence lifetime down to 10 ps [13].

In order to detect individual molecules diffusing in solution at high concentration, a special must be taken to ensure reducing the background fluorescence from molecules a few tens of nanometers away from the plasmonic antenna, yet still in the confocal detection volume. At the physiologically-relevant concentrations of a few micromolar, several thousands of molecules that are still present within the diffraction-limited confocal volume, and their non-enhanced emission can overwhelm the enhanced single-molecule signal from the nanoscale plasmonic hotspot. Specific strategies have been developed to address this issue, using low quantum yield emitters and/or adding a metal cladding layer. The design termed “antenna-in-box” combines a gap-antenna inside a nano-aperture, and has enabled single molecule detection at concentrations above 20 μM together with fluorescence enhancement above a thousand-fold (Fig. 1b) [14, 15].

Enhanced fluorescence spectroscopies applications need nanoantennas featuring a large-scale availability together with narrow gaps accessible to target the fluorescent probes. Recent advances in top-down lithography have been achieved towards this goal, using blurring-free stencil lithography patterning by dry etching through nanostencils [25] or a combination of electron-beam lithography followed by planarization, etch back and template stripping [15].

3.2 Bottom-up self assembly

Bottom-up assembly of nanoparticles offers an attractive alternative to classical top-down nanofabrication thanks to its low operation cost, narrow gap sizes, use of single crystalline structures and potential large-scale availability [26, 27]. A simple and direct approach relies on using a single nanoparticle of the shape of a sphere [28, 29, 30, 31, 32] or nanorod [18, 19, 33]. Taking advantage of the local surface plasmon resonance enhancing and confining the electromagnetic field within a few nanometers near the nanorod apex, fluorescence enhancement above a thousand fold could be obtained with an antenna as simple as a single nanorod (Fig. 1c) [18, 19], enabling fluorescence correlation spectroscopy at high concentrations [33]. Drying of nanoparticle colloidal suspension provides another straightforward access to resonant optical antennas with nanometer gap sizes [34]. For a dimer of 80 nm gold nanoparticles with 6 nm gap, 600-fold fluorescence enhancement and detection volumes down to 70 zL were achieved [35]. It is worth also mentioning that ultrafast emission of quantum dots down to picosecond lifetimes was achieved thanks to a patch antenna realized by a silver nanocube on a gold surface [36, 37, 38].

To provide a better control on the nanogap distance and provide more reproducible antennas, the self-assembly of metal nanoparticles can be templated by DNA double strands [39, 40, 41, 42, 43] or DNA origami [16, 17, 44, 45]. This latter approach constitutes a powerful method to assemble nanoparticles into complex 3D designs with gap size tunability (Fig. 1d). It also brings the key ability to bind the desired target molecule at the antenna hot spot [16]. Recent results use 100 nm diameter nanoparticles assembled on a DNA origami pillar with 12-17 nm gap featuring a binding site for a single fluorescent molecule. Fluorescence enhancement up to 5000-fold were reported, together with single-molecule detection at concentrations up to 25 μM [17].

3.3 Dielectric alternatives to plasmonic metals

The metals conventionally used for plasmonics (gold, silver, aluminum) still have significant absorption losses in the visible spectral range used for fluorescence spectroscopy applications. Energy damping to the free electron gas in the metal can severely quench the fluorescence emission, while simultaneously absorption of the laser beam induce Joule heating of the nanostructure [10]. To find an alternative featuring lower absorption losses, all-dielectric nanoantennas based on silicon or germanium have been recently introduced [46, 47, 48, 49]. Planar concentrators have been used to achieve extremely high collection efficiencies and detection rates of a single fluorescent molecule [50, 51]. Silicon nanogap antennas (with a design very close to their gold counterpart) have been reported to enhance the fluorescence of a dye layer [52, 53] and of single molecules [54], with single molecule enhancement factors up to 270-fold. Although the gains reported remain lower than for the plasmonic metal counterparts, this approach is a promising alternative compatible with CMOS processing.

To conclude this section, Figure 2 compares the figure of merit for the single molecule fluorescence enhancement (defined as $\eta_F \times \phi$) for different techniques. As the techniques develop further and further, the figure of merit rises up to values around 300 which represent the current state-of-the-art at the end of 2017.

4 Biochemical applications of enhanced fluorescence

In this section, we discuss two driving applications for antenna-enhanced single molecule fluorescence detection: real-time DNA sequencing and living cell membrane investigations at the nanoscale. We also present the emerging field of single molecule Förster resonance energy transfer (smFRET) enhanced by nanoantennas.

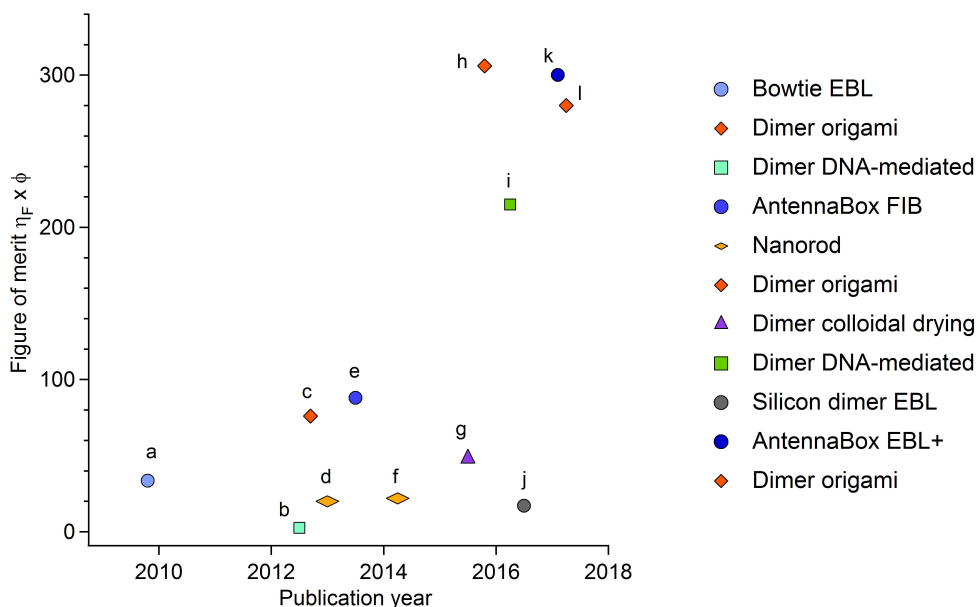


Figure 2: Figure of merit for the single molecule fluorescence enhancement (defined as the product of the measured fluorescence enhancement factor η_F times the initial quantum yield ϕ of the fluorescent emitter used) as a function of the publication year for different nanoantenna designs and fabrication approach. The letters written next to the data points relate to the following references: a [13], b [41], c [16], d [18], e [14], f [19], g [35], h [17], i [43], j [54], k [15], l [45].

4.1 Real-time DNA sequencing

Achieving personalized quantitative genomics requires the development of novel methods for DNA and RNA sequencing that enable high-throughput, high-accuracy and low operating costs. Monitoring real-time single-molecule DNA and RNA sequencing by a single polymerase enzyme is a promising approach. So far, it has been achieved using circular nanoholes milled in an aluminum film (also called zero-mode waveguides [4]) [55, 56]. Each nanohole provides an observation chamber for watching the activity of a single polymerase enzyme at micromolar concentration of fluorescently-tagged oligonucleotides, each base (A,T,G,C) is color-coded with a spectrally distinct fluorophore. Every time a fluorescent nucleotide is incorporated into the DNA strand, there is a burst of fluorescence of millisecond duration which allows to retrieve the corresponding sequence as the replication is performed. A few thousand of nanoholes are currently monitored simultaneously, enabling massive parallelization [55]. So far, only circular aluminum nanoholes have been used for this application, but the sensitivity and detection rates could greatly benefit from the higher fluorescence enhancement offered by plasmonic nanoantennas.

4.2 Nanoscale organization of lipid membranes

Recent progress in cell biology indicates that the cell membrane features transient and fluctuating nanoscale assemblies of sterol and sphingolipids known as lipid rafts [57]. Investigating the role and formation of these nanodomains is of key interest for cell biology. However, the nanometer and microsecond resolutions that are simultaneously required fall far beyond the reach of standard microscopes [58]. With their ability to confine light into nanometer dimensions and drastically improve the fluorescence signal from a single molecule, optical nanoantennas offer a promising approach to investigate the nanoscale dynamic organization of living cell membranes [59, 60, 61, 62, 63]. The flat geometry of the lipid bilayer membrane is remarkably well suited for the investigation by planar nanoantenna designs. Demonstrations on model lipid membranes [62] and CHO cell membranes [63] highlight the potential of nanoantennas to reveal nanodomains of 10 nm dimensions and sub-millisecond characteristic times. This fully bio-compatible approach opens interesting opportunities for living cell biophysics with single-molecule sensitivity at ultrahigh spatial and temporal resolutions.

4.3 Förster resonance energy transfer FRET

As we have seen, optical nanoantennas can enhance the fluorescence signal from single quantum emitters. Interestingly, they can also be applied to enhance and modify the Förster resonance energy transfer (FRET) between two nearby fluorescent emitters. FRET is one of the most widely used single molecule fluorescence techniques, with many applications to investigate the conformation dynamics of large molecules [64] or perform biosensing [65]. Metal nanoapertures [66, 67] and nanogap antennas [68, 69, 70] have been shown to significantly enhance the FRET rate while simultaneously enabling single-molecule FRET at micromolar concentrations. Interestingly, the FRET gain is larger for more distant donor and acceptor molecules, which is interesting for the investigation of biochemical structures with donor-acceptor distances much beyond the classical Förster radius [66, 68]. Moreover, the strongly inhomogeneous electromagnetic fields in plasmonic nanoantennas was also demonstrated to enhance FRET between nearly perpendicular donor and acceptor dipoles, enabling FRET detection that would otherwise be forbidden in a homogeneous confocal volume [70].

5 Conclusion

Optical nanoantennas overcome the classical diffraction limits of confocal microscopes and confine light down to dimensions close to the size of a single molecule. This enables to drastically improve the fluorescence emission rate, notably for low quantum yield emitters. Thanks to the recent advances in the nanofabrication, either top-down or bottom-up, the single molecule fluorescence toolbox is now significantly expanded. New directions involve single molecule fluorescence dynamics studies

at physiologically-relevant micromolar concentrations and living cell membrane studies at ultrahigh spatiotemporal resolutions. The potential of nanoantennas is at hand to reveal new information on biological functions and dynamics.

References

- [1] Holzmeister, P.; Acuna, G. P.; Grohmann, D.; Tinnefeld, P. Breaking the concentration limit of optical single-molecule detection. *Chem. Soc. Rev.* **2013**, *43*, 1014-1028.
- [2] Punj, D.; Ghenuche, P.; Moparthi, S. B.; de Torres, J.; Grigoriev, V.; Rigneault, H.; Wenger, J. Plasmonic antennas and zero-mode waveguides to enhance single molecule fluorescence detection and fluorescence correlation spectroscopy toward physiological concentrations. *WIREs Nanomed. Nanobiotechnol.*, **2014**, *6*, 268-282.
- [3] Novotny, L., Hecht, B. *Principles of Nano-Optics*. Cambridge University Press, Cambridge (2006).
- [4] Levene, M.J.; Korlach, J.; Turner, S.W.; Foquet, M.; Craighead, H.G.; Webb, W. W. Zero-mode waveguides for single-molecule analysis at high concentrations. *Science* **2003**, *299*, 682-686.
- [5] Moran-Mirabal, J. M.; Craighead, H. G. Zero-mode waveguides: Sub-wavelength nanostructures for single molecule studies at high concentrations. *Methods* **2008**, *46*, 11-17.
- [6] Wenger, J. ; H. Rigneault, H. Photonic Methods to Enhance Fluorescence Correlation Spectroscopy and Single Molecule Fluorescence Detection. *Int. J. Mol. Sci.* **2010**, *11*, 206-221.
- [7] Novotny, L.; van Hulst, N. Antennas for light. *Nat. Photonics* **2011**, *5*, 83-90.
- [8] Schuller, J. A., Barnard, E. S., Cai, W. S., Jun, Y. C., White, J. S. ; Brongersma, M. L. Plasmonics for extreme light concentration and manipulation. *Nat. Materials* **2010**, *9*, 193-204.
- [9] Biagioni, P.; Huang, J. S.; Hecht, B. Nanoantennas for visible and infrared radiation. *Rep. Prog. Phys.* **2012**, *75*, 024402.
- [10] Lakowicz, J.; Fu, Y. Modification of single molecule fluorescence near metallic nanostructures. *Laser Photonics Rev.* **2009**, *3*, 221-232
- [11] Halas, N. J.; Lal, S.; Chang, W. S.; Link, S.; Nordlander, P. Plasmons in strongly coupled metallic nanostructures. *Chem. Rev.* **2011**, *111*, 3913-3961.
- [12] Koenderink, A. F. Single-photon nanoantennas. *ACS Photonics* **2017**, *4*, 710-722.

- [13] Kinkhabwala, A.; Yu, Z. F.; Fan, S. H.; Avlasevich, Y.; Mullen, K.; Moerner, W. E. Large single-molecule fluorescence enhancements produced by a bowtie nanoantenna. *Nat. Photonics* **2009**, *3*, 654-657.
- [14] Punj, D.; Mivelle, M.; Moparthy, S.B.; van Zanten, T.S.; Rigneault, H.; van Hulst, N.F.; García-Parajo, M.F.; Wenger, J. A plasmonic ‘antenna-in-box’ platform for enhanced single-molecule analysis at micromolar concentrations. *Nat. Nanotechnol.* **2013**, *8*, 512-516.
- [15] Flauraud, V.; Regmi, R.; Winkler, P. M.; Alexander, D. T. L.; Rigneault, H.; van Hulst, N. F.; García-Parajo, M. F.; Wenger, J.; Brugger, J. In-Plane Plasmonic Antenna Arrays with Surface Nanogaps for Giant Fluorescence Enhancement. *Nano Lett.* **2017**, *17*, 1703-1710.
- [16] Acuna, G. P.; Möller, F. M.; Holzmeister, P.; Beater, S.; Lalkens, B.; Tinnefeld, P. Fluorescence Enhancement at Docking Sites of DNA-Directed Self-Assembled Nanoantennas. *Science* **2012**, *338*, 506-510.
- [17] Puchkova, A.; Vietz, C.; Pibiri, E.; Wünsch, B.; Sanz Paz, M.; Acuna, G. P.; Tinnefeld, P. DNA Origami Nanoantennas with over 5000-Fold Fluorescence Enhancement and Single-Molecule Detection at 25 μ M. *Nano Lett.* **2015**, *15*, 8354-8359.
- [18] Yuan, H.; Khatua, S.; Zijlstra, P.; Yorulmaz, M.; Orrit, M. Thousand-fold enhancement of single-molecule fluorescence near a single gold nanorod. *Angew. Chem.* **2013**, *125*, 1255–1259.
- [19] Khatua, S.; Paulo, P. M. R.; Yuan, H.; Gupta, A.; Zijlstra, P.; Orrit, M. Resonant Plasmonic Enhancement of Single-Molecule Fluorescence by Individual Gold Nanorods. *ACS Nano* **2014**, *8*, 4440-4449.
- [20] Zander, C.; Enderlein, J.; Keller, R. A. (Eds.), *Single-Molecule Detection in Solution - Methods and Applications*, (VCH-Wiley, Berlin/New York, 2002).
- [21] Lakowicz, J. R. *Principles of fluorescence spectroscopy*, 3rd Edition (Springer, Berlin/New York, 2006).
- [22] Gill, R.; Tian, L.; Somerville, W. R. C.; Le Ru, E. C.; van Amerongen, H.; Subramaniam, V. Silver Nanoparticle Aggregates as Highly Efficient Plasmonic Antennas for Fluorescence Enhancement. *J. Phys. Chem. C* **2012**, *116*, 16687-16693.
- [23] Wenger, J. Fluorescence Enhancement Factors on Optical Antennas: Enlarging the Experimental Values without Changing the Antenna Design, *Int. J. Optics* **2012**, *2012*, 828121.
- [24] Kinkhabwala, A. A.; Yu, Z. F.; Fan, S. H.; Moerner, W. E. Fluorescence correlation spectroscopy at high concentrations using gold bowtie nanoantennas. *Chem. Phys.* **2012**, *406*, 3–8.

- [25] Flauraud, V.; van Zanten, T.S.; Mivelle, M.; Manzo, C.; García-Parajo, M.F.; Brugger, J. Large-Scale Arrays of Bowtie Nanoaperture Antennas for Nanoscale Dynamics in Living Cell Membranes. *Nano Lett.* **2015**, *15*, 4176–4182.
- [26] Grzelczak, M.; Vermant, J.; Furst, E. M.; Liz-Marzán, L. M. Directed self-assembly of nanoparticles. *ACS Nano* **2010**, *4*, 3591–3605.
- [27] Edel, J. B.; Kornyshev, A. A.; Urbakh, M. Self-assembly of nanoparticle arrays for use as mirrors, sensors, and antennas. *ACS Nano* **2013**, *7*, 9526–9532.
- [28] Estrada, L. C.; Aramendia, P. F.; Martinez, O. E. 10000 times volume reduction for fluorescence correlation spectroscopy using nano-antennas. *Opt. Express* **2008**, *16*, 20597–20602.
- [29] Wang, Q.; Lu, G.; Hou, L.; Zhang, T.; Luo, C.; Yang, H.; Barbillon, G.; Lei, F.E.; Marquette, C.A.; Perriat, P.; Tillement, O.; Roux, S.; Ouyang, Q.; Gong, Q. Fluorescence correlation spectroscopy near individual gold nanoparticle. *Chem. Phys. Lett.* **2011**, *503*, 256–261.
- [30] Lu, G. W.; Liu, J.; Zhang, T. Y.; Li, W. Q.; Hou, L.; Luo, C. X.; Lei, F.; Manfait, M.; Gong, Q. H. Plasmonic near-field in the vicinity of a single gold nanoparticle investigated with fluorescence correlation spectroscopy. *Nanoscale* **2012**, *4*, 3359–3364.
- [31] Choudhury, S. D.; Ray, K.; Lakowicz, J. R. Silver nanostructures for fluorescence correlation spectroscopy: reduced volumes and increased signal intensities. *J. Phys. Chem. Lett.* **2012**, *3*, 2915–2919.
- [32] Punj, D.; de Torres, J.; Rigneault, H.; Wenger, J. Gold nanoparticles for enhanced single molecule fluorescence analysis at micromolar concentration. *Opt Express* **2013**, *21*, 27338–27343.
- [33] Khatua, S.; Yuan, H.; Orrit, M. Enhanced-fluorescence correlation spectroscopy at micro-molar dye concentration around a single gold nanorod. *Phys. Chem. Chem. Phys.* **2015**, *17*, 21127–21132.
- [34] Fan, J.A.; Wu, C.; Bao, K.; Bao, J.; Bardhan, R.; Halas, N.J.; Manoharan, V.N.; Nordlander, P.; Shvets, G.; Capasso, F. Self-assembled plasmonic nanoparticle clusters. *Science* **2010**, *328*, 1135–1138.
- [35] Punj, D.; Regmi, R.; Devilez, A.; Plauchu, R.; Moparthi, S. B.; Stout, B.; Bonod, N.; Rigneault, H.; Wenger, J. Self-assembled nanoparticle dimer antennas for plasmonic-enhanced single-molecule fluorescence detection at micromolar concentrations. *ACS Photonics* **2015**, *2*, 1099–1107.

- [36] Akselrod, G. M.; Argyropoulos, C.; Hoang, T. B.; Ciraci, C.; Fang, C.; Huang, J.; Smith, D. R.; Mikkelsen, M. H. Probing the mechanisms of large Purcell enhancement in plasmonic nanoantennas. *Nat. Photonics* **2014**, *8*, 835-840.
- [37] Hoang, T. B.; Akselrod, G. M.; Argyropoulos, C.; Huang, J. N.; Smith, D. R.; Mikkelsen, M. H. Ultrafast spontaneous emission source using plasmonic nanoantennas. *Nat. Commun.* **2015**, *6*, 7788.
- [38] Hoang, T. B.; Akselrod, G. M.; Mikkelsen, M. H. Ultrafast Room-Temperature Single Photon Emission from Quantum Dots Coupled to Plasmonic Nanocavities. *Nano Lett.* **2016**, *16*, 270-275.
- [39] Fan, J. A.; He, Y.; Bao, K.; Wu, C.; Bao, J.; Schade, N.B.; Manoharan, V. N.; Shvets, G.; Nordlander, P.; Liu, D.; Capasso, F. DNA-enabled self-assembly of plasmonic nanoclusters. *Nano Lett.* **2011**, *11*, 4859-4864.
- [40] Busson, M. P.; Rolly, B.; Stout, B.; Bonod, N.; Larquet, E.; Polman, A.; Bidault, S. Optical and topological characterization of gold nanoparticle dimers linked by a single DNA double strand. *Nano Lett.* **2011**, *11*, 5060-5065.
- [41] Busson, M. P.; Rolly, B.; Stout, B.; Bonod, N.; Bidault, S. Accelerated single photon emission from dye molecule-driven nanoantennas assembled on DNA. *Nature Commun.* **2012**, *3*, 962.
- [42] Busson, M.P.; Rolly, B.; Stout, B.; Bonod, N.; Wenger, J.; Bidault, S. Photonic engineering of hybrid metal-organic chromophores. *Angew. Chem. Int. Ed.* **2012**, *51*, 11083-11087.
- [43] Bidault, S.; Devilez, A.; Maillard, V.; Lermusiaux, L.; Guigner, J.-M.; Bonod, N.; Wenger, J. Picosecond lifetimes with high quantum yields from single-photon emitting colloidal nanostructures at room temperature. *ACS Nano* **2016**, *10*, 4806-4815.
- [44] Zhang, T.; Gao, N.; Li, S.; Lang, M.J.; Xu, Q.H. Single-Particle Spectroscopic Study on Fluorescence Enhancement by Plasmon Coupled Gold Nanorod Dimers Assembled on DNA Origami, *J. Phys. Chem. Lett.* **2015**, *6*, 2043-2049.
- [45] Vietz, C.; Kaminska, I.; Sanz Paz, M.; Tinnefeld, P.; Acuna, G. P. Broadband Fluorescence Enhancement with Self-Assembled Silver Nanoparticle Optical Antennas. *ACS Nano* **2017**, *11*, 4969-4975.
- [46] Garcia-Etxarri, A.; Gomez-Medina, R.; Froufe-Perez, L. S.; Lopez, C.; Chantada, L.; Scheffold, F.; Aizpurua, J.; Nieto-Vesperinas, M.; Saenz, J. J. Strong magnetic response of submicron silicon particles in the infrared. *Opt. Express* **2011**, *19*, 4815-4826.

- [47] Evlyukhin, A. B.; Novikov, S. M.; Zywiets, U.; Eriksen, R. L.; Reinhardt, C.; Bozhevolnyi, S. I.; Chichkov, B. N. Demonstration of magnetic dipole resonances of dielectric nanospheres in the visible region. *Nano Lett.* **2012**, *12*, 3749-3755.
- [48] Kuznetsov, A. I.; Miroshnichenko, A. E.; Fu, Y. H.; Zhang, J.; Lukyanchuk, B. Magnetic light. *Sci. Rep.* **2012**, *2*, 492.
- [49] Albella, P.; Poyli, M. A.; Schmidt, M. K.; Maier, S. A.; Moreno, F.; Saenz, J. J.; Aizpurua, J. Low-loss electric and magnetic field-enhanced spectroscopy with subwavelength silicon dimers. *J. Phys. Chem. C* **2013**, *117*, 13573-13584.
- [50] Lee, K. G.; Chen, X. W.; Eghlidi, H.; Kukura, P.; Lettow, R.; Renn, A.; Sandoghdar, V.; Göttinger, S. A planar dielectric antenna for directional single-photon emission and near-unity collection efficiency. *Nat. Photonics* **2011**, *5*, 166-169.
- [51] Chu, X.-L.; Brenner, T.; Chen, X.-W.; Ghosh, Y.; Hollingsworth, J.; Sandoghdar, V.; Göttinger, S. Experimental realization of an optical antenna designed for collecting 99% of photons from a quantum emitter. *Optica* **2014**, *1*, 203-208.
- [52] Caldarola, M.; Albella, P.; Cortes, E.; Rahmani, M.; Roschuk, T.; Grinblat, G.; Oulton, R. F.; Bragas, A. V.; Maier, S. A. Non-plasmonic nanoantennas for surface enhanced spectroscopies with ultra-low heat conversion. *Nat. Commun.* **2015**, *6*, 7915.
- [53] Cambiasso, J.; Grinblat, G.; Li, Y.; Rakovich, A.; Cortes, E.; Maier, S. A. Bridging the Gap between Dielectric Nanophotonics and the Visible Regime with Effectively Lossless Gallium Phosphide Antennas. *Nano Lett.* **2017**, *17*, 1219-1225.
- [54] Regmi, R.; Berthelot, J.; Winkler, P. M.; Mivelle, M.; Proust, J.; Bedu, F.; Ozerov, I.; Begou, T.; Lumeau, J.; Rigneault, H.; Garcia-Parajo, M. F.; Bidault, S.; Wenger, J.; Bonod, N. All-Dielectric Silicon Nanogap Antennas To Enhance the Fluorescence of Single Molecules, *Nano Lett.* **2016**, *16*, 5143-5151.
- [55] Eid, J.; Fehr, A.; Gray, J.; Luong, K.; Lyle, J.; Otto, G.; Peluso, P.; Rank, D.; Baybayan, P.; Bettman, B.; Bibillo, A.; Bjornson, K.; Chaudhuri, B.; Christians, F.; Cicero, R.; Clark, S.; Dalal, R.; deWinter, A.; Dixon, J.; Foquet, M.; Gaertner, A.; Hardenbol, P.; Heiner, C.; Hester, K.; Holden, D.; Kearns, G.; Kong, X.; Kuse, R.; Lacroix, Y.; Lin, S.; Lundquist, P.; Ma, C.; Marks, P.; Maxham, M.; Murphy, D.; Park, I.; Pham, T.; Phillips, M.; Roy, J.; Sebra, R.; Shen, G.; Sorenson, J.; Tomaney, A.; Travers, K.; Trulson, M.; Vieceli, J.; Wegener, J.; Wu, D.; Yang, A.; Zaccarin, D.; Zhao, P.; Zhong, F.; Korlach, J.; Turner, S. Real-Time DNA Sequencing from Single Polymerase Molecules. *Science* **323**, 133-138 (2009).

- [56] Uemura, S.; Aitken, C. E.; Korlach, J.; Flusberg, B. A.; Turner, S. W.; Puglisi, J. D. Real-time tRNA transit on single translating ribosomes at codon resolution, *Nature* **464**, 1012-1017(2010).
- [57] Sezgin, E.; Levental, I.; Mayor, S.; Eggeling, C. The mystery of membrane organization: composition, regulation and roles of lipid rafts. *Nat. Rev. Mol. Cell Biol.*, **2017**, *18*, 361-374.
- [58] Eggeling, C.; Ringemann, C.; Medda, R.; Schwarzmann, G.; Sandhoff, K.; Polyakova, S.; Belov, V. N.; Hein, B.; von Middendorff, C.; Schönle, A.; Hell, S. W. Direct Observation of the Nanoscale Dynamics of Membrane Lipids in a Living Cell. *Nature*, **2009**, *457*, 1159-1162.
- [59] Lohmüller, T.; Iversen, L.; Schmidt, M.; Rhodes, C.; Tu, H. L.; Lin, W. C.; Groves, J. T. Single molecule tracking on supported membranes with arrays of optical nanoantennas. *Nano Lett.* **2012**, *12*, 1717-1721.
- [60] Flynn, J. D.; Haas, B. L.; Biteen, J. S. Plasmon-Enhanced Fluorescence from Single Proteins in Living Bacteria. *J. Phys. Chem. C* **2017**, *120*, 20512-20517.
- [61] Pradhan, B.; Khatua, S.; Gupta, A.; Aartsma, T.; Canters, G.; Orrit, M. Gold-Nanorod-Enhanced Fluorescence Correlation Spectroscopy of Fluorophores with High Quantum Yield in Lipid Bilayers. *J. Phys. Chem. C* **2016**, *120*, 25996-26003.
- [62] Winkler, P. M.; Regmi, R.; Flauraud, V.; Brugger, J.; Rigneault, H.; Wenger, J.; García-Parajo, M. F. Transient Nanoscopic Phase Separation in Biological Lipid Membranes Resolved by Planar Plasmonic Antennas, *ACS Nano*, **2017**, *11*, 7241-7250.
- [63] Regmi, R.; Winkler, P. M.; Flauraud, V.; Borgman, K. J. E.; Manzo, C.; Brugger, J.; Rigneault, H.; Wenger, J.; García-Parajo, M. F. Planar Optical Nano-Antennas Resolve Cholesterol-Dependent Nanoscale Heterogeneities in the Plasma Membrane of Living Cells, *Nano Lett.*, DOI: 10.1021/acs.nanolett.7b02973.
- [64] Weiss S. Measuring conformational dynamics of biomolecules by single molecule fluorescence spectroscopy. *Nat. Struct. Biol.* **2000**, *7*, 724-729.
- [65] Medintz, I. L.; Clapp, A. R.; Mattoussi, H.; Goldman, E. R.; Fisher, B.; Mauro, J. M. Self-assembled nanoscale biosensors based on quantum dot FRET donors. *Nat. Materials* **2003**, *2*, 630-638.
- [66] Ghenuche, P.; de Torres, J.; Moparthi, S. B.; Grigoriev, V.; Wenger, J. Nanophotonic Enhancement of the Förster Resonance Energy Transfer Rate with Single Nanoapertures. *Nano Lett.* **2014**, *14*, 4707-4714.

- [67] de Torres, J.; Ghenuche, P.; Moparthi, S. B.; Grigoriev, V.; Wenger, J. FRET Enhancement in Aluminum Zero-Mode Waveguides. *Chem. Phys. Chem.* **2015**, *16*, 782-788.
- [68] Ghenuche, P.; Mivelle, M.; de Torres, J.; Moparthi, S. B.; Rigneault, H.; Van Hulst, N. F.; Garcia-Parajo, M.F.; Wenger, J. Matching Nanoantenna Field Confinement to FRET Distances Enhances Förster Energy Transfer Rates. *Nano Lett.* **2015**, *15*, 6193-6201.
- [69] Bidault, S.; Devilez, A.; Ghenuche, P.; Stout, B.; Bonod, N.; Wenger, J. Competition between Förster resonance energy transfer and donor photodynamics in plasmonic dimer nanoantennas. *ACS Photonics* **2016**, *3*, 895-903.
- [70] de Torres, J.; Mivelle, M.; Moparthi, S. B.; Rigneault, H.; Van Hulst, N. F.; Garcia-Parajo, M. F.; Margeat, E.; Wenger, J. Plasmonic Nanoantennas Enable Forbidden Förster Dipole-Dipole Energy Transfer and Enhance the FRET Efficiency, *Nano Lett.* **2016**, *16*, 6222-6230.